

## Article

# The Potential Role of S- and Fe-Cycling Bacteria on the Formation of Fe-Bearing Mineral (Pyrite and Vivianite) in Alluvial Sediments from the Upper Chicamocha River Basin, Colombia

Claudia Patricia Quevedo <sup>1</sup>, Juan Jiménez-Millán <sup>2,\*</sup>, Gabriel Ricardo Cifuentes <sup>1</sup>, Antonio Gálvez <sup>3</sup> , José Castellanos-Rozo <sup>4</sup> and Rosario Jiménez-Espinosa <sup>2</sup> 

- <sup>1</sup> Faculty of Sciences and Engineering, Water Resources Research Group, University of Boyacá, Tunja 15000, Colombia; patriciaquevedo@uniboyaca.edu.co (C.P.Q.); grcifuentes@uniboyaca.edu.co (G.R.C.)
- <sup>2</sup> Department of Geology and CEACTEMA, University of Jaén, Campus Las Lagunillas, 23071 Jaén, Spain; respino@ujaen.es
- <sup>3</sup> Microbiology Division, Department of Health Sciences, Campus Las Lagunillas, 23071 Jaén, Spain; agalvez@ujaen.es
- <sup>4</sup> Department of Biology and Microbiology, Faculty of Sciences and Engineering, Environmental Management Group, University of Boyacá, Tunja 150003, Colombia; joscastellanos@uniboyaca.edu.co
- \* Correspondence: jmillan@ujaen.es



**Citation:** Quevedo, C.P.; Jiménez-Millán, J.; Cifuentes, G.R.; Gálvez, A.; Castellanos-Rozo, J.; Jiménez-Espinosa, R. The Potential Role of S- and Fe-Cycling Bacteria on the Formation of Fe-Bearing Mineral (Pyrite and Vivianite) in Alluvial Sediments from the Upper Chicamocha River Basin, Colombia. *Minerals* **2021**, *11*, 1148. <https://doi.org/10.3390/min11101148>

Academic Editors: Anna Panyushkina and Maxim Muravyov

Received: 15 September 2021

Accepted: 15 October 2021

Published: 18 October 2021

**Publisher's Note:** MDPI stays neutral with regard to jurisdictional claims in published maps and institutional affiliations.



**Copyright:** © 2021 by the authors. Licensee MDPI, Basel, Switzerland. This article is an open access article distributed under the terms and conditions of the Creative Commons Attribution (CC BY) license (<https://creativecommons.org/licenses/by/4.0/>).

**Abstract:** S- and Fe-cycling bacteria can decisively affect the crystallization of Fe-bearing minerals in sediments from fluvial environments. We have studied the relationships between the Fe-bearing mineral assemblage and the bacterial community composition in the sediments rich in organic matter from the upper Chicamocha river basin (Colombia). Rapid flowing sections of the river contain sediments that have a high redox potential, are poor in organic matter and are enriched in kaolinite and quartz. On the other hand, the mineral assemblage of the sediments deposited in the La Playa dam with a high content in organic matter is enriched in Fe-bearing minerals: (a) vivianite and pyrite in the permanently flooded sediments of the dam and (b) pyrite and goethite in the periodically emerged sediments. The bacterial community composition of these sediments reveals anthropic organic matter pollution processes and biodegradation associated with eutrophication. Moreover, periodically emerged sediments in the La Playa dam contain bacterial groups adapted to the alternation of dry and wet periods under oxic or anoxic conditions. Cell-shaped aggregates with a pyritic composition suggest that sulfate-reducing bacteria (SRB) communities were involved in the precipitation of Fe-sulfides. The precipitation of vivianite in the flooded sediments was favored by a greater availability of Fe(II), which promoted the iron-reducing bacteria (IRB) enrichment of the sediments. The presence of sulfur-oxidizing bacteria (SOB) in the flooded sediments and the activity of iron-oxidizing bacteria (IOB) in the periodically emerged sediments favored both pyrite crystallization under a high sulfide availability and the oxidation of microbially precipitated monosulfides. Moreover, IOB enhanced goethite formation in the periodically emerged sediments.

**Keywords:** vivianite; pyrite; goethite; bacterial community; Chicamocha river

## 1. Introduction

Alluvial sediments deposited in river systems heavily used by anthropic activities can act as sinks for contaminants affecting the geochemistry of P, S and Fe in river courses and alluvial sediments (see e.g., [1–3]). Nutrient and pollutant loads can influence the accumulation of organic matter, sediment–water interactions, redox conditions and microbial activity in alluvial systems, which control mineralogical and biogeochemical processes that affect the fate of these elements [3].

The construction of dams that regulate water outflow has been used as a tool for the remediation of pollution problems of these elements in river courses [4,5]. These reservoirs can modify the composition of the river waters through dilution with rainwater [6].

Phosphate is an important pollutant of these waters and is associated with the use of fertilizers and detergents [7]. One of the main effects associated with phosphate pollution is the eutrophication of water bodies, such as those produced by damming, giving rise to the spread of algae, water properties degradation and a decrease in oxygen availability [3,8]. These processes can lead to the deposit of clay sediments rich in organic matter [9]. The high organic matter contents and the reducing conditions generated in these environments promote mineral reactions related to biological activity, frequently controlling the mobility of P, S and Fe.

The redox reactions of Fe-bearing minerals in organic matter and clay-rich sediments have a strong effect on the speciation, mobility and bio-availability of pollutants [10]. The precipitation of iron in different minerals depends on the environmental conditions. Redox conditions are one of the main factors controlling the precipitation of Fe-bearing minerals, favoring the precipitation of Fe(II)-minerals (mainly phosphates and sulfides) under high redox potential conditions and Fe(III)-minerals (mainly oxides and oxyhydroxides) under high redox potential conditions. In anoxic environments rich in P and S, microbial processes can promote the formation of vivianite ( $\text{Fe}_3(\text{PO}_4)_2 \cdot 8\text{H}_2\text{O}$ ) and iron sulfide minerals, such as mackinawite ((Fe,Ni)S) or pyrite ( $\text{FeS}_2$ ). The crystallization of sulfide minerals can widely affect all of these reactions. Pyrite is the most representative mineral of the framboids, which is commonly described in the organic matter interstices [11]. This textural position evidences the importance of organic matter for pyrite crystallization favored by the microbial sulfate reduction. Iron oxides and oxyhydroxides (e.g., goethite or hematite) are the predominant Fe-bearing minerals in oxic systems [12], even when the environment is eutrophicated by the enrichment in phosphate [13].

Water reservoirs are periodically discharged to the river. Periodical water discharges create areas with intermittently emerged sediments, whereas other areas contain permanently flooded sediments, producing important changes in the redox conditions of sediments. When the reservoir is drained, the redox conditions in the sediments can fluctuate according to the humidity conditions [14]. Therefore, the water level on the sediments can be an important factor controlling the sediment redox conditions. If sediments are repeatedly flooded and drained, wetting and drying periods alternate, which can be related with changes in the redox status affecting the biogeochemical processes of sediments [15]. However, the influence of these processes on the dynamics of the bacterial communities involved in redox reactions is not well known yet [14,16].

The presence of sulfate-reducing bacteria (SRB) that use sulfate to degrade organic matter under anaerobic conditions [17] and produce  $\text{H}_2\text{S}$ , which can react with metals to fix them as sulfide minerals [18], is common in sediments deposited in lakes and rivers [19]. Therefore, SRB can capture metal ions into low-solubility metal sulfides that remove environmental toxic pollutants [20–22].

The oxidation of reduced sulfide to sulfate by sulfur-oxidizing bacteria (SOB) can release some of the metals retained in sulfide minerals [17]. Therefore, the activity of SRB and SOB have important effects on the sulfur biogeochemistry [17,23], controlling the equilibrium of the sulfur cycle [17] and influencing the transformations of metals in sediments and waters. Thus, the process of metal removal from water and sediments by mineral crystallization is frequently mediated by SRB [24], which can be strengthened by the activity of iron-reducing bacteria (IRB), which transform Fe(III) to Fe(II), affecting the availability of metals in sediments and soils [15]. On the other hand, the oxidation of crystallized reduced sulfide by the SOB action can, once again, favor the liberation of metals to the environment [17]. Watanabe et al. [14] suggested that the frequent changes in the redox conditions of materials where wetting and drying periods alternate can facilitate iron-oxidizing bacteria (IOB) to participate in the oxidation of Fe in soils.

This study provides a set of mineralogical data to reveal sediments with an accumulation of Fe-bearing minerals at 25 sites within the upper Chicamocha river basin (UCRB) alluvial system. We investigated the distribution of phosphates, sulfides and oxyhydroxides in the organic matter and clay-rich sediments deposited in a river segment of the UCRB

(Paipa, Colombia) with slow-flowing conditions and periodic flooding produced by the La Playa dam. We aim to evaluate the role of S- and Fe-cycling bacteria in the distribution of these minerals in the sediments and their influence on P, S and Fe immobilization in sediments deposited in the La Playa dam, trying to identify the main microbial communities associated with the biogeochemical processes that influence mineral precipitation. We have combined mineralogical and microbiological methods to explain the presence of Fe-bearing phosphates, sulfides and oxyhydroxides in eutrophicated organic-matter-rich sediments.

## 2. Background Context

The area of study (UCRB) belongs to the equatorial Andes (Colombia, Boyacá department) (Figure 1). Fluvial plains that are around 2500 m of altitude above sea level can be found in this area. The length of the UCRB is 62.46 km, its average slope is 0.12% and it flows to the Caribbean Sea [25]. The annual rainfall of the UCRB oscillates from 650–1200 mm and the average year temperature is 13.1 °C.

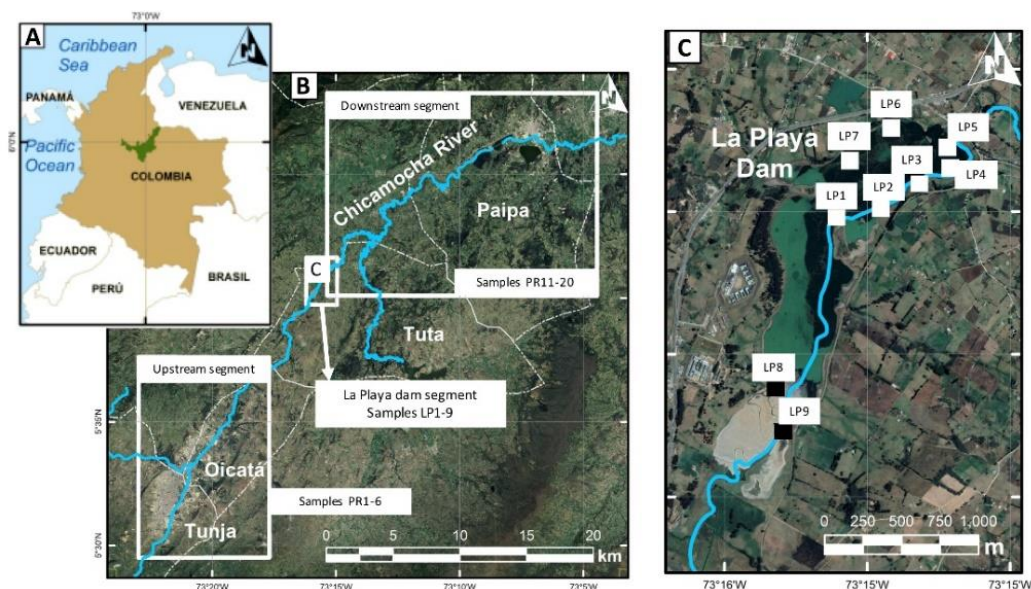


**Figure 1.** Study area and location of samples: (A) global map of the region; (B) studied segments from the Chicamocha River; (C) detail of the La Playa segment.

The most relevant anthropic change in the UCRB is the La Playa dam, which divides the UCRB into three segments: a central segment with slow-flowing conditions and two fast-flowing sections situated downstream and upstream of the dam (Figure 1). The reservoir of the La Playa dam receives wastewaters (urban sewage) from the towns of the region and waters of the agricultural activities, which generate a high nutrient load and intense eutrophication [26].

Fast flowing sections of the Chicamocha river show sediments enriched in quartz and kaolinite with low contents in organic matter (TOC < 0.52%), a high redox potential (around 70 mV) and low electrical conductivity (around 200  $\mu\text{S}/\text{cm}$ ) [27]. The sediments from the La Playa dam are characterized by alternating bands of microlaminated organic-matter-rich layers and clay-rich layers [27], showing a high organic matter content (TOC of up to 11.1%), low redox potential (around  $-230$  mV) and high electrical conductivity (2625  $\mu\text{S}/\text{cm}$ ) [27]. Fe-bearing minerals were exclusively found in sediments from the La Playa dam and were absent from the rest of the alluvial sediments from the Chicamocha river basin [9,27].

The quantitative chemical composition and mineral composition of the untreated samples of the studied sediments in the La Playa dam, as well as their in situ physicochemical properties, are shown in Table 1.

**Table 1.** Sediment characterization of La Playa sediments. Major element sediment compositions of the untreated samples determined by XRF (X-ray fluorescence spectroscopy), loss of ignition (LOI), content in total organic carbon (TOC) and mineral abundances determined by XRD (in weight percentage, except for S in mg/kg). In situ physicochemical properties. R.P.: redox potential (mV); E.C.: electrical conductivity ( $\mu\text{S}/\text{cm}$ ); Qz: quartz; Py: pyrite; Viv: vivianite; Gth: goethite.

Sample	SiO <sub>2</sub>	Al <sub>2</sub> O <sub>3</sub>	FeO	S	LOI	TOC	Clay	Qz	Py	Viv	Gth	pH	R.P.	E.C.
LP 1	61.34	19.21	4.21	27201	17.21	14.51	44	44	7	5	-	7.0	-54	1431
LP 2	60.83	18.74	4.38	24534	18.34	14.88	42	50	5	<5	-	7.0	-32	1254
LP 3	62.71	17.62	4.75	23244	16.99	13.99	42	48	5	5	-	7.1	-21	1572
LP 4	60.32	19.23	3.88	18321	17.61	14.76	46	43	6	5	-	7.2	-31	1423
LP 5	61.12	18.31	4.04	26523	18.44	14.41	43	48	5	<5	-	7.0	-12	1621
LP 6	60.21	17.21	3.89	17453	15.33	13.80	47	46	5	<5	-	6.9	-27	1599
LP 7	63.24	18.24	4.11	21956	10.51	4.29	45	46	5	6	-	7.0	-32	1324
LP 8	61.31	15.99	3.81	11345	16.22	11.00	45	42	7	-	6	7.0	-5	2431
LP 9	60.18	17.22	4.38	15781	15.43	13.80	43	45	5	-	7	7.0	2	1854

### 3. Materials and Methods

#### 3.1. Materials

A network with 25 points of sediment sampling through the three segments of the UCRB was designed (Figure 1). Sediment cores were obtained with a stainless Shelby tube. Hanna Instruments meters for sediments and soils (HI98168 and HI98168) were used to determine in situ sediment pH, redox potential and electrical conductivity, respectively. The samples of sediment were dried at 40 °C in an oven as a previous step for other mineralogical treatments.

#### 3.2. Mineralogical Methods

Random and oriented aggregates were used to obtain XRD data. An isodynamic magnetic separator was used to obtain a fraction of the total sample enriched in Fe-bearing minerals. A Panalytical X'Pert Pro diffractometer (CuK $\alpha$  radiation, 45 kV, 40 mA) (CICT of the Universidad de Jaén, Jaén, Spain) equipped with a X'Celerator solid-state linear detector was used to acquire the diffraction patterns (step increment 0.008° 2 $\theta$ , counting time 10 s/step).

Field emission scanning electron microscope (FESEM, Merlin Carl Zeiss, Oberkochen, Germany) was used for textural and chemical characterization of sediments. Back-scattered electron (BSE) images were obtained from polished sections. We used secondary electron (SE) images for the study of sediment fragments. Elemental mineral composition was obtained with energy dispersive X-ray spectrometry (EDX).

High resolution transmission electron microscopy (HRTEM) study was carried out in selected samples in a HAADF FEI TITAN G2 microscope operated at 300 kV (CIC, University of Granada, Granada, Spain). Samples were deposited on coated Au and Cu grids. Nanoparticle qualitative analyses were acquired by energy-dispersive X-ray spectroscopy (EDX) in the mode scanning transmission electron microscope.

#### 3.3. Microbiological Methods

A DNeasy PowerSoil Kit (Quiagen, Barcelona, Spain) was used for DNA extraction from the samples following the instructions of the manufacturer. A QuantiFluor® ONE dsDNA system (Promega, Madison, USA) was employed to determine the quality and the amount of the obtained DNA. The DNA was stored at -20 °C until analysis. Regarding DNA sequencing and analysis, 16S rDNA gene amplicons were obtained following the 16S rDNA gene Metagenomic Sequencing Library Preparation Illumina protocol (Cod. 15044223 Rev. A). The gene-specific sequences used in this protocol targeted the 16S rDNA gene V3 and V4 region. Illumina adapter overhang nucleotide sequences were added to the gene-specific sequences. The primers were selected from Klindworth et al. [28]. The following 16S rDNA gene amplicon PCR primer sequences were used: forward primer, 5'TCGTCGGCAGCGTCAGATGTGTATAAGAGACAGCC-

TACGGGNGGCWGCAG3'; reverse primer, 5'GTCTCGTGGGCTCGGAGATGTGTATAA-GAGACAGGACTACHVGGTATCTAATCC3'. Microbial genomic DNA (5 ng/ $\mu$ L in 10 mM Tris pH 8.5) was used to initiate the protocol. After 16S rDNA gene amplification, the multiplexing step was performed using a Nextera XT Index Kit (FC-131-1096) (Illumina, Cambridge, UK). One  $\mu$ L of the PCR product was run on a Bioanalyzer DNA 1000 chip to verify the size (expected size  $\sim$ 550 bp). Following size verification, the libraries were sequenced using a  $2 \times 300$  pb paired-end run (MiSeq Reagent kit v3 (MS-102-3001)) on a MiSeq Sequencer according to the manufacturer's instructions (Illumina, Cambridge, UK). Quality assessment was performed with the use of the prinseq-lite program [29]. The sequence data were analyzed using the qiime2 pipeline [30]. Denoising, paired-end joining and chimera depletion were performed, starting with paired-end data using the DADA2 pipeline [31]. Taxonomic affiliations were assigned using the Naive Bayesian classifier integrated in the qiime2 plugins and the SILVA\_release\_132 database [32]. Statistical analysis was carried out with SPSS software version 24 (IBM Corp., Foster City, CA, USA). The sequencing output files will be available at the Sequence Read Archive (SRA) service of the European Bioinformatics Institute (EBI) database under Accession Number PRJEB47878.

## 4. Results

### 4.1. Fe-Bearing Minerals of the Sediments

Fe-bearing minerals are absent in the fast-flowing sections of the UCRB (Samples PR, Figure 1). On the contrary, the mineral assemblage of the La Playa dam is rich in clay minerals and characterized by the abundance of kaolinite, illite-dioctahedral vermiculite mixed layers (I-DV), framboids pyrite, vivianite and goethite (Figure 2) [9]. Disrupted organic matter microbands alternate with clay-rich microlaminae (Figure 3A) in permanently flooded sediments and periodically emerged materials of the dam.

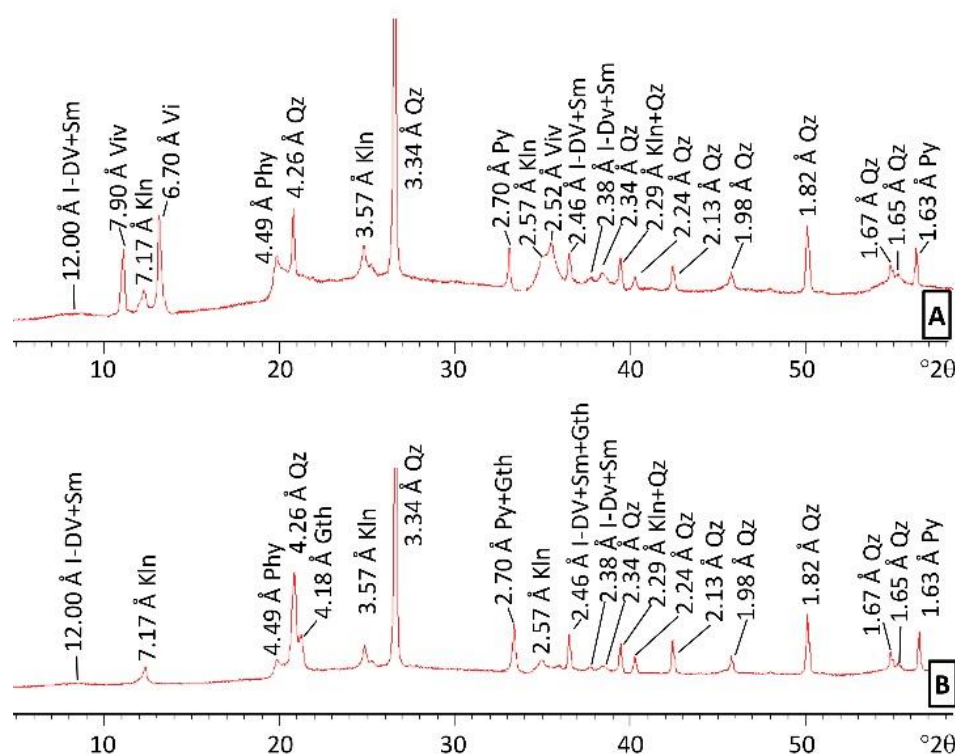


**Figure 2.** Selected XRD patterns from sediments of La Playa dam: (A) permanently flooded sediments (sample LP7); (B) periodically emerged sediments (sample LP8). I-DV: illite-smectite mixed layers; Sm: smectite; Kln: kaolinite; Viv: vivianite; Phy: phyllosilicates; Qz: quartz; Py: pyrite; Gth: goethite.

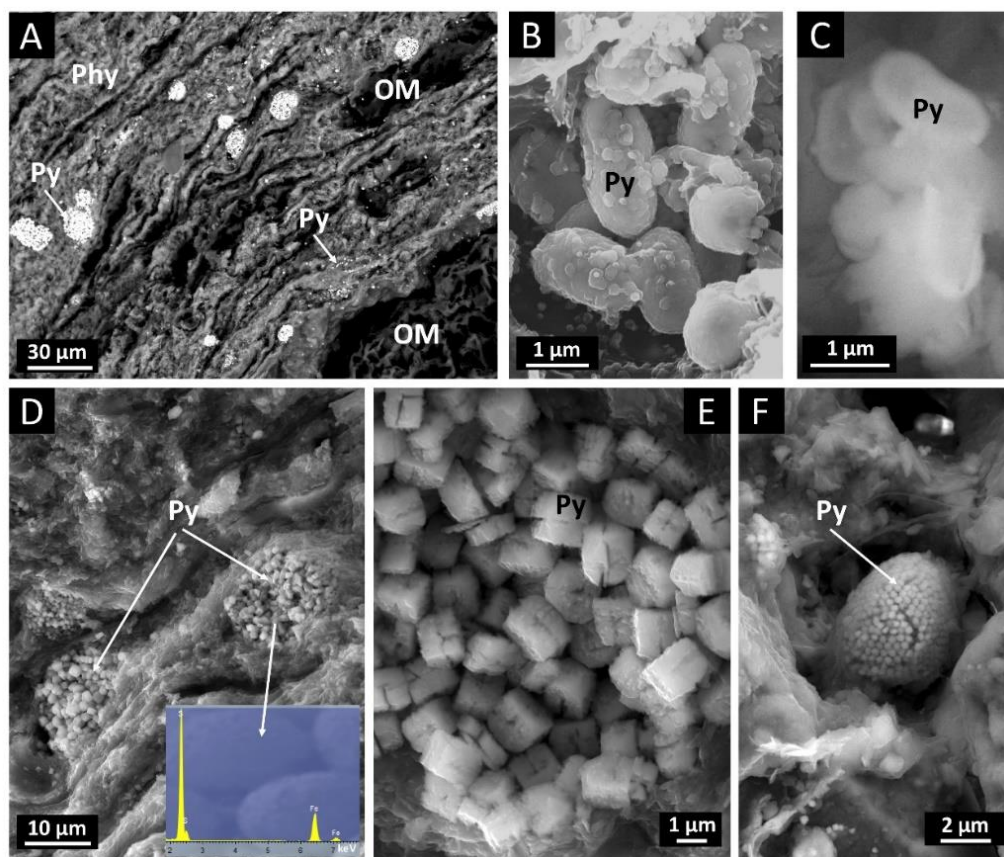


**Figure 3.** FESEM and EDX images of pyrite from sediments of La Playa dam: (A) disrupted organic matter microbands alternating with clay-rich microlaminae (BSE image)(sample LP7); (B,C) pyrite cell-shape aggregates (sample LP7); (D) pyrite framboids from permanently flooded sediments (sample LP7); (E) pyrite hopper crystals from permanently flooded sediments (sample LP7); (F) pyrite microframboids with honeycomb disposition crystals in periodically emerged sediments (sample LP8). Phy: phyllosilicates; Py: pyrite; OM: organic matter.

Pyrite can be identified by 2.70 and 1.63 Å XRD peaks in both types of sediments (Figure 2). SEM images revealed the presence of dispersed nanocrystals forming cell-shaped aggregates (Figure 3A–C), as well as framboids that are up to 20 μm in size surrounded by lamination made of hopper crystals (Figure 3D,E) in permanently flooded sediments and smaller microframboids (<5 μm) containing regular nanocrystals with a honeycomb disposition in periodically emerged sediments (Figure 3F).

XRD patterns indicated that the presence of vivianite is restricted to the permanently flooded sediments (6.70 and 2.52 Å peaks, Figure 2A). Vivianite appears as small prismatic to flat nanocrystals frequently associated with the occurrence of plant fragments (Figure 4A,B). HRTEM images and EDX elemental mapping revealed the presence of crystals with a vivianite composition (Figure 4C–F) and lattice fringes around 6.7 Å, which can be produced by the (020) spacing of vivianite.

Goethite was only identified in the XRD patterns of the periodically emerged sediments by a small peak at 4.18 Å and a peak at 2.46 Å over-imposed to clays (Figure 2B). The SEM images revealed that goethite occurs as crusts with dendritic and botryoidal morphologies in the silicate-rich bands of the sediments (Figure 5).

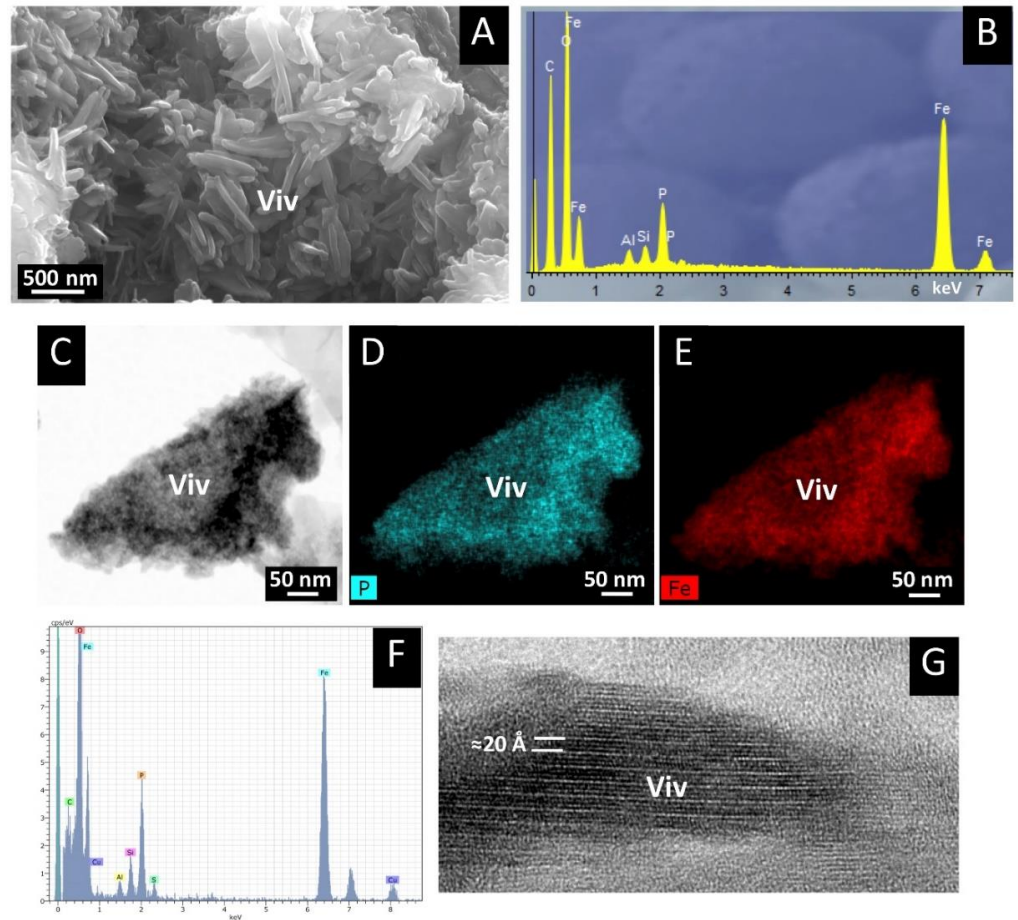


**Figure 4.** FESEM, HRTEM and EDX images of vivianite from permanently flooded sediments of La Playa dam (sample LP7): (A) prismatic to flat nanocrystals of vivianite frequently associated with the occurrence of plant fragments (SE image); (B) FESEM-EDX spectrum of vivianite from (A); and (C) HRTEM image (bright field) of a vivianite crystal; (D) elemental map (HRTEM-EDX) of P (image c); (E) elemental map (HRTEM-EDX) of Fe (image c); (F) HRTEM-EDX spectrum of vivianite; (G) lattice fringe image of vivianite crystal from image (C). Viv: vivianite.

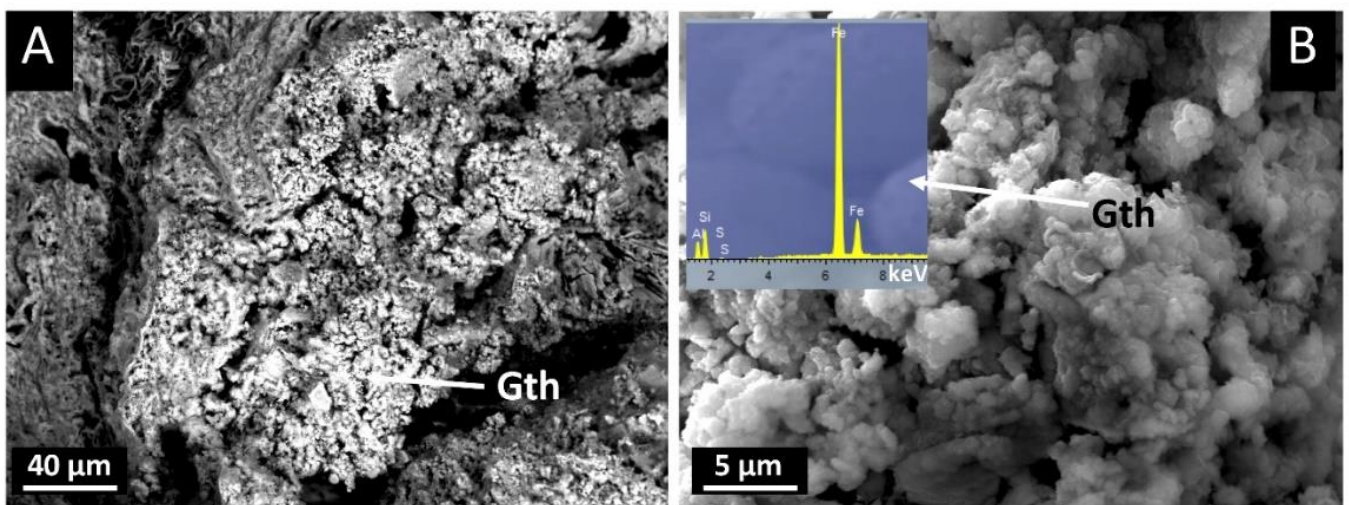


**Figure 5.** FESEM and EDX images of goethite from periodically emerged sediments of La Playa dam ((A) sample LP8, (B) sample LP9). Gth: goethite.

#### 4.2. Bacterial Populations

*Proteobacteria* were very abundant in all of the studied samples (25–29%). *Rhodanobacter*, *Geobacter*, *Aquabacterium*, *Dechloromonas*, *Pseudomonas*, *Dyella*, *Desulfomicrobium* and *Desulfobulbus* are the most abundant genera of this phylum in the permanently flooded sediments (3.6–0.7%), whereas the periodically emerged sediments are characterized by the presence of order *Elsterales*, families *Micropepsaceae*, *Acetobacteraceae*, *Gallionellaceae* (including genus *Sideroxydans*) and genera *Syntrophobacter*, *Acidibacter*, *Desulfobacca* and *Thauera* (3.5–0.8%) (Figure 6). Due to the high bacterial diversity of the studied sediments, and given that Figure 6 only shows groups with a relative abundance of at least 1%, the percentage of diversity represented in Figure 6 oscillates between 53–65%.

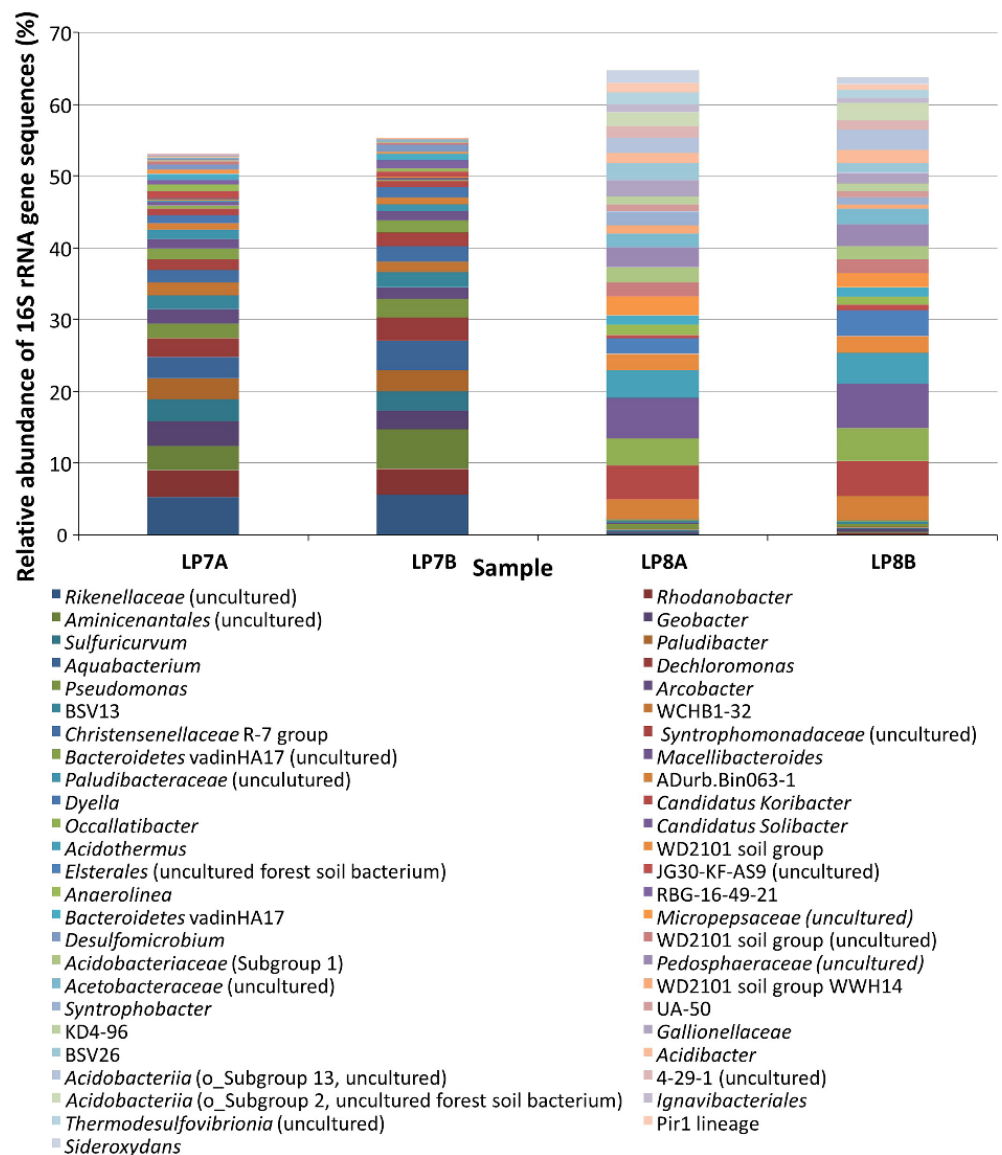


**Figure 6.** Bacterial diversity in the organic matter-rich sediments from La Playa dam. LP7A and LP7B are samples that are permanently flooded. LP8A and LP8B are samples that are periodically emerged. “A samples” belong to the surficial part of the core sediment, whereas “B samples” were taken from the deepest part of the core sediment in LP7 and LP8 sampling points. 16S rRNA sequences with a relative abundance of at least 1% are shown. Sequences were assigned to genus level or the corresponding higher taxonomic group.

The abundance of other phyla depends on the type of sediments analyzed. Important differences can be observed between the permanently flooded and the periodically emerged sediments of the dam.

High representations of *Bacteroidetes* (28%) and *Firmicutes* (12%) were observed in the permanently flooded sediments of the dam. *Rikenellaceae* family members are the best-represented communities of *Bacteroidetes* (around 5%). Other *Bacteroidetes* genera documented in these sediments were WCHB1-32, BVS13 and *Macellibacteroides* and *Paludibacter*. The phylum *Firmicutes* is represented by the *Christensenellaceae* family and *Syntrophomonadaceae* members in the flooded sediments. Significant amounts of *Epsilonbacteraeota* phyla (around 5%) are also identified in these sediments, with genera *Sulfuricurvum* and *Arcobacter* as the main representative communities.

Samples that are periodically emerged and dried in the La Playa dam are characterized by higher contents of members of the *Acidobacteria* (27%, *Candidatus Koribacter* and *Candidatus Solibacter*), *Verrucomicrobia* (8%), *Planctomycetes* (8%), *Chloroflexi* (8%, including *Anaerolineaceae* up to 7.7%), *Actinobacteria* (6%) and *Nitrospirae* (4%, including *Thermodesulfovibrionia* community) phyla. The phylum *Bacteroidetes* is represented less in the periodically emerged sediments than in the permanently flooded sediments (up to 12%), with families *Bacteroidetes* vadinHA17, UA-50, BSV26 and *Ignavibacteriales* order as the main communities of this phylum.

## 5. Discussion

### 5.1. Mineral Distribution

The mineral distribution is related to the two main types of materials that can be distinguished in the La Playa dam. Pyrite is present in all of the sediments deposited in the reservoir. Quevedo et al. [9,27] indicated that the enrichment in the clay minerals and organic matter (TOC up to 13.84%) of the sediments from the La Playa reservoir, with regard to the quartz-rich sediments from the rest of the sediments of the UCRB, favored the precipitation of sulfide minerals.

However, the spatial distribution of Fe-bearing phosphate and hydroxide in the sediments of the La Playa dam seems to be associated with the flooding conditions of the sediments. Permanently flooded sediments that are richer in organic matter and have a lower redox potential (around  $-230\text{mV}$ ) [27] from the northern part of the reservoir are characterized by the presence of vivianite and, by contrast, periodically emerged sediments from the southern part of the reservoir with lower organic matter contents (4.29%) and higher Eh values ( $-10\text{mV}$ ) contain goethite. These data suggest that redox conditions and the organic matter content are two important factors controlling the formation of the Fe-bearing minerals of the sediments.

Pyrite and vivianite were found together in the flooded sediments of the La Playa reservoir, which is relatively uncommon in natural sediments (see e.g., [33]). The presence of pyrite is very common in anoxic sediments formed in sulfate-rich water environments. Pyrite exhibited two types of morphologies in the studied sediments. On the one hand, the presence of small dispersed crystals forming encrusted cell-shaped aggregates (Figure 4B,C) suggests the importance of microorganisms in the nucleation of sulfide minerals. On the other hand, the formation of microframboids, including hopper pyrite crystals, suggests transformation processes under high supersaturation values of Fe and sulfide, which promote the fast accumulation of growth units at the crystal edges, causing the typical faces of hopper grains [34].

Pyrite formation can compete with the precipitation of vivianite for the available reduced Fe of the environment, avoiding vivianite crystallization when the concentration of sulfide is very high [35]. Iron can act on the immobilization of phosphorous under anoxic conditions through the biotic and abiotic precipitation of Fe(II) vivianite in highly eutrophized environments [36–38]. Indeed, vivianite is considered as a main phosphorus sink in natural and engineered environments [39–41]. Rothe et al. [36] suggested that vivianite authigenesis is mainly controlled by the ratio between sulfide and Fe(II) availability. Thus,

the formation of vivianite is frequently restricted to environments where an excess of Fe in dissolution is available after the crystallization of sulfides. However, microorganisms can play an important role in the availability of these substances and, therefore, in the concomitant crystallization of phosphates and sulfides [37]. In the next section, we explore some relationships between the mineral distribution and the presence of microorganisms in the sediments.

The Fe-bearing minerals in the periodically emerged sediments from the La Playa dam were goethite and pyrite. When the dam is drained, as a result, a modification of the moisture conditions is produced, which can lead to the fluctuation of the redox conditions in the sediments. Therefore, the variation of the water level is an important factor in regulating the sediment redox conditions and can affect the iron redox cycle, which is considered as a crucial factor for controlling the biogeochemistry of organic-matter-rich sediments. Watanabe et al. [14] showed that repeated cycles of wetting and drying produced a significant oscillation of the iron redox status of soils. The presence of goethite in the periodically emerged sediments suggests that processes of Fe oxidation occurred. Druschel et al. [42] indicated that iron oxidation kinetics are mainly affected by oxygen availability, although pH, temperature, the surface area of the Fe<sup>(III)</sup> bearing minerals and the presence of iron-oxidizing microorganisms can influence the rate of the process. Cornell and Schwertmann [12] indicated that iron oxides/oxyhydroxides are prevalent in oxic sediments; even those deposited in eutrophic environments [13]. The formation of Fe<sup>(III)</sup> can affect the stability of the rest of the Fe-bearing minerals in the sediments. Duverger et al. [38] suggested that the presence of ferric iron can promote the conversion of mackinawite, favoring the pyrite enrichment of the sediments.

### 5.2. The Role of the Bacterial Communities

Sediments that are rich in organic matter from the La Playa dam (Chicamocha River Basin, Colombia) are characterized by a bacterial community with a diverse composition. Processes of organic matter degradation and mineral transformation in the C, Fe, P and S cycles are associated with the bacterial activity of the dam sediments.

The permanently flooded sediments of the dam are characterized by the high amount of *Bacteroidetes* and *Firmicutes* phyla. Most of the bacterial communities from these groups identified in this type of sediment have been documented in the biodegradation of organic matter deposits from anthropogenic activities in sediments from dams that favors endogenous water pollution and eutrophication, which is a potential threat for the pond environment [43–45]. The high representation of the *Rikenellaceae* family (*Bacteroidetes*) in these sediments can be associated with being responsible for the decomposition of harmful algal bloom in ponds [43]. The rest of *Bacteroidetes* genera identified in these sediments, such as WCHB1-32, BVS13 and *Macellibacteroides* [16], have been thought to be important in the formation of methanogenic precursors from organic matter degradation. Hou et al. [46] suggested that members of the phylum *Firmicutes*, such as the *Christensenellaceae* family, are frequently reported in human feces and other animal feces, and show a fairly high capability for degrading carbohydrates and carboxylic acids. Within the phylum *Firmicutes*, the presence of relevant amounts of *Syntrophomonadaceae* members in the flooded sediments from the La Playa dam can contribute to produce H<sub>2</sub> used by sulfate-reducing bacteria (SRB) acting as syntrophic partners [47].

On the other hand, in samples that are periodically emerged and dried in the La Playa dam, several members of the phylum *Acidobacteria*, such as *Candidatus Koribacter* and *Candidatus Solibacter*, are very well represented in this type of sediment from the La Playa dam. These groups have been reported in high amounts in organic-matter-rich soils from dry seasons that are affected by fertirrigation practices [48] and have a high salinity [49]. Other bacterial groups described in soils and sediments rich in organic matter with a high salinity, such as members of the *Verrucomicrobia* (see e.g., [49]) and *Actinobacteria* [50,51], were also enriched in the periodically emerged sediments from the La Playa dam. Berg et al. [35] indicated that *Actinobacteria* have a mostly aerobic style of life.

This is also consistent with the enrichment in the *Planctomycetes* phylum of these sediments (7.7%). Dedysh et al. [52] indicated that these bacteria are able to colonize oxic peat layers from boreal and subarctic wetlands. Regardless, the periodically emerged sediments are also characterized by the presence of significant amounts of *Anaerolineaceae* from the *Chloroflexi* phylum (up to 7.7%), which are anaerobic organisms with the capability of fermentation [53]. The abundance of these communities can be related to anoxic conditions and high organic matter contents. Cifuentes et al. [54] suggested that *Anaerolineaceae* and *Bacteroidetes\_vadinHA17* are important communities involved in the final degradation stages of organic matter in sulfidic zones. The presence of the *Ignavibacteriales* order in the periodically emerged sediments can be related to CO<sub>2</sub> fixation processes [55].

Lin et al. [53] indicated that *Anaerolineaceae* can act as biogeochemical linkers that relate the reactions of C and S in mangrove sediments, favoring the mobility of these elements in the system, which can affect the cycle of Fe and other metals of the sediments and the activity of iron- and sulfur-cycling bacteria, sulfur- and sulfate-reducing bacteria (SRB), sulfide-oxidizing bacteria (SOB), iron-reducing bacteria (IRB) and iron-oxidizing bacteria (IOB). SRB, SOB, IRB and IOB communities have been reported in the La Playa dam sediments, but their distributions are not homogeneous.

SRB are present in all of the organic matter rich sediments from La Playa. Flooded sediments contain *Pseudomonas* (up to 2.9%), *Desulfomicrobium* and *Desulfobulbus* (up to 1%) genera. Hazra et al. [56] documented that *Pseudomonas* plays an important role in the synthesis of spherical ZnS nanoparticles. Moreover, this bacterial group is characterized by its elevated levels of metal resistance [57] and its ability to colonize in sewage [58] and remove organic carbon in the wetland ponds [59]. Liu et al. [60] indicated that *Pseudomonas* are responsible for the hydrocarbon degradation of sediments coupled to the reaction of Fe reduction in sediments. Rigorously anaerobic SRB *Desulfomicrobium* and *Desulfobulbus* have been reported as microorganisms that are involved in sulfate reduction, promoting P release at contaminated sediments [60].

On the contrary, predominant SRB communities in periodically emerged sediments are *Syntrophobacter* (up to 1.9%), *Thermodesulfovibrionia* (up to 1.7%) and *Desulfobacca* (0.8%). Li et al. [61] reported that *Syntrophobacter* are SRB that are frequently present in sulfate-rich wetlands. Gessink et al. [62] indicated that *Thermodesulfovibrionia* play a crucial role in the cycles of nitrogen and sulfur in groundwaters. *Desulfobacca* is commonly found in sludge environments and paddy soils [63].

IRB are very well represented in the flooded sediments where the *Proteobacteria* genera *Geobacter* (3%), *Dechloromonas* (3%) and *Pseudomonas* (2%), as well as the *Bacteroidetes* genus *Paludibacter* (3%), are present. Wang et al. [63] documented that the presence of *Geobacter* and *Paludibacter* was associated with organic-matter-rich sediments with humic acids, playing an essential function in the release of Fe(II) to the interstitial waters of sediments under anaerobic conditions. *Dechloromonas* has been found to be related to the reduction of Fe(III) to Fe(II) in sludges that contain P and Fe, promoting the reaction of Fe(II) with PO<sub>4</sub><sup>3-</sup> to form vivianite [41]. Moreover, Zhang et al. [64] indicated that the genus *Dechloromonas* is frequently associated with phosphate accumulations and that high phosphate contents favor its growth. Berg et al. [35] showed the presence of *Pseudomonas* as one of the IRB in the Lake Pavin water column. Liu et al. [60] indicated that *Pseudomonas* can play an active role in the connection of the carbon cycle with the Fe reductions reactions in hydrocarbon-rich sediments. Sanchez-Andrea et al. [65] described *Paludibacter* as a fermentative microorganism in high sulfate and metal concentration environments that is able to transfer electrons from anaerobic oxidations to promote the reduction of iron.

In contrast, *Acidibacter* (up to 2%) is the only IRB genus reported in the periodically emerged sediments of the La Playa dam. This genus has been classified as acidophilic, with the capability of reducing dissolved Fe(III) in low pH and high Fe environments [66].

IOB are absent in the flooded sediments, but members of the *Gallionellaceae* family (2%) and the *Sideroxydans* genus (up to 1.9%) are very well represented in the periodically emerged sediments of the La Playa dam. Watanabe et al. [14] revealed the importance of

bacteria that belong to the *Gallionellaceae* family and the *Sideroxydans* genus on the oxidation of Fe(II) in soils that alternate wetting and drying periods, reporting that the amount of IOB was higher in the surface oxic layer of these types of soils. Berg et al. [35] identified the presence of the obligately aerobic to microaerobic iron oxidizer *Gallionella* sequences in anoxic waters, because they can be adapted to low oxygen levels.

In flooded sediments of the La Playa dam, two genera of anaerobic SOB, *Sulfuricurvum* (around 3%) and *Arcobacter* (up to 2%), were detected. However, these groups of bacteria were absent in the periodically emerged sediments. Berg et al. [35] observed that *Sulfuricurvum* was the dominant SOB under elevated free sulfide concentrations. Zhang et al. [67] suggested that the presence of *Arcobacter* can be used as an indicator of sewer and human fecal pollution.

Duverger et al. [38] revealed that the SOB presence could increase the pyrite crystallization rate, suggesting that the SRB-induced formation of pyrite can be enhanced by the SOB simultaneous activity.

## 6. Conclusions

1. The high content in bacterial communities from the *Bacteroidetes* and *Firmicutes* phyla of the permanently flooded sediments of the La Playa dam reveal anthropic organic matter pollution processes (e.g., the presence of groups commonly found in feces, such as the *Christensenellaceae* family) and biodegradation associated with eutrophication (*Rikenellaceae* family, WCHB1-32, BVS13 and *Macellibacteroides*);
2. The composition of the bacterial communities of the periodically emerged and dried sediments in the La Playa dam is characterized by the presence of groups frequently reported in high salinity soils (*Verrucomicrobia* and *Actinobacteria*) affected by the alternation of dry and wet periods (*Candidatus Koribacter* and *Candidatus Solibacter*) with oxic conditions (*Planctomycetes*), as well as by the presence of anaerobic microorganisms related to anoxic conditions (*Anaerolineaceae*);
3. Both flooded and periodically emerged sediments show relevant SRB communities involved in the precipitation of Fe-sulfides (Figure 7). SEM images showing cell-shaped aggregates with a pyritic composition support the importance of the bacterial communities in the nucleation and transformation of sulfide minerals. The activity of these bacterial groups in the flooded sediments can be reinforced by syntrophic partners to produce H<sub>2</sub> used by SRB (*Syntrophomonadaceae*) and increase the sulfide availability;

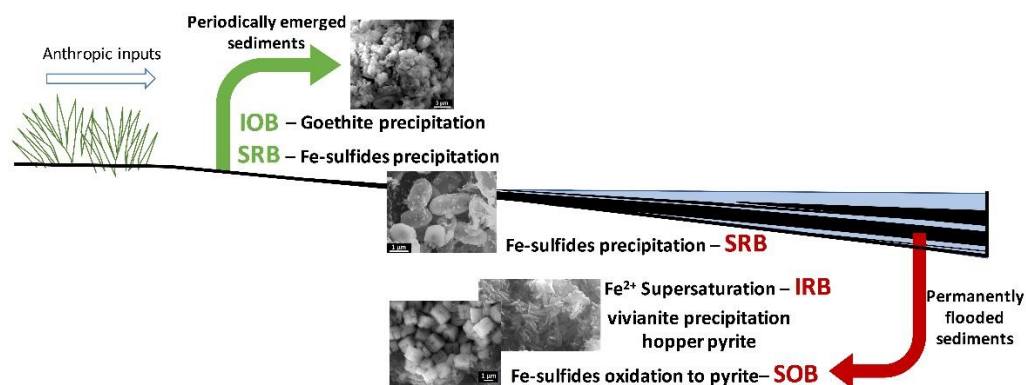


**Figure 7.** Bacterial groups and mineral precipitation in the organic-matter-rich sediments from La Playa dam. SRB: sulfate-reducing bacteria; IRB: iron-reducing bacteria; SOB: sulfur-oxidizing bacteria; IOB: iron-oxidizing bacteria.

4. IRB enrichment in the permanently flooded sediments of the La Playa dam and the presence of IOB in the periodically emerged sediments promotes a greater availability of Fe(II) in the flooded sediments, which favors the precipitation of vivianite by the contribution of microbial iron- and sulfur-reducing processes;

5. Bacterial activity should favor supersaturation in Fe(II) (promoted by IRB and SRB) and sulfide (stimulated by SRB and their syntrophic partners that produce H<sub>2</sub>), which can be associated with the crystallization of hopper pyrite crystals in the permanently flooded sediments;
6. Moreover, the SOB presence in the flooded sediments and the presence of Fe(III) due to aerobic conditions and the activity of IOB in the periodically emerged sediments can favor both pyrite crystallization under a high sulfide availability and the oxidation of microbially precipitated monosulfides. Moreover, IOB could enhance the precipitation of goethite in the periodically emerged sediments, even under low oxygen levels.

**Author Contributions:** C.P.Q. and G.R.C. conducted field observations and sampling. J.J.-M., R.J.-E., C.P.Q. and G.R.C. performed mineralogical characterization. A.G. and J.C.-R. carried out the characterization of the bacterial communities. All of the authors discussed the analytical results and prepared the manuscript. All authors have read and agreed to the published version of the manuscript.

**Funding:** This work has been financed by the Spanish research project PGC2018-094573-B-I00 from the MCIU-AEI-FEDER, research group RNM-325 of the Junta de Andalucía (Spain), research project FEDER-UJA 2020 ref 1380934 and research project PAIDI P20-00990 from the Junta de Andalucía. Our gratitude is also extended to Asociación Universitaria Iberoamericana de Posgrado (AUIP) and the Universidad de Boyacá. Additional thanks to Colombian Research groups Gestión Ambiental COL0005468 and Gestión de Recursos Hídricos COL0005477.

**Data Availability Statement:** Not applicable.

**Conflicts of Interest:** The authors declare no conflict of interest. The funders had no role in the design of the study; in the collection, analyses or interpretation of data; in the writing of the manuscript, or in the decision to publish the results.

## References

1. Noël, V.; Boye, K.; Kukkadapu, R.K.; Bone, S.; Pacheco, J.S.L.; Cardarelli, E.; Janot, N.; Fendorf, S.; Williams, K.H.; Bargar, J.R. Understanding controls on redox processes in floodplain sediments of the Upper Colorado River Basin. *Sci. Total Environ.* **2017**, *603–604*, 663–675. [[CrossRef](#)] [[PubMed](#)]
2. Andrade, G.R.P.; Cuadros, J.; Partiti, C.M.S.; Cohen, R.; Vidal-Torrado, P. Sequential mineral transformation from kaolinite to Fe-illite in two Brazilian mangrove soils. *Geoderma* **2018**, *309*, 84–99. [[CrossRef](#)]
3. Li, R.; Gao, L.; Wu, Q.; Liang, Z.; Hou, L.; Yang, Z.; Chen, J.; Jiang, T.; Zhu, A.; Li, M. Release characteristics and mechanisms of sediment phosphorus in contaminated and uncontaminated rivers: A case study in South China. *Environ. Pollut.* **2021**, *268*, 115749. [[CrossRef](#)] [[PubMed](#)]
4. Willis, C.M.; Griggs, G.B. Reductions in fluvial sediment discharge by coastal dams in California and implications for beach sustainability. *J. Geol.* **2003**, *111*, 167–182. [[CrossRef](#)]
5. Khadse, G.K.; Meshram, D.B.; Deshmukh, P.; Labhasetwar, P.K. Water quality of Tehri dam reservoir and contributing rivers in the Himalayan region. *India. Sustain. Water Resour. Manag.* **2019**, *5*, 1951–19616. [[CrossRef](#)]
6. Cifuentes, G.R.; Jiménez-Espinosa, R.; Jiménez-Millán, J.; Quevedo, C.P. Damming induced natural attenuation of hydrothermal waters by runoff freshwater dilution and sediment biogeochemical transformations (Sochagota Lake, Colombia). *Water* **2021**, in press.
7. Azam, H.M.; Finneran, K.T. Fe(III) reduction mediated phosphate removal as vivianite (Fe<sub>3</sub>(PO<sub>4</sub>)<sub>2</sub>·8H<sub>2</sub>O) in septic system wastewater. *Chemosphere* **2014**, *97*, 1–9. [[CrossRef](#)]
8. Kokocinski, M.; Dziga, D.; Spoof, L.; Stefaniak, K.; Jurczak, T.; Mankiewicz-Boczek, J.; Meriluoto, J. First report of the cyanobacterial toxin cylindrospermopsin in the shallow, eutrophic lakes of western Poland. *Chemosphere* **2009**, *74*, 669–675. [[CrossRef](#)]
9. Quevedo, C.P.; Jiménez-Millán, J.; Cifuentes, G.R.; Jiménez-Espinosa, R. Clay mineral transformations in anthropic organic matter-rich sediments under saline water environment. Effect on the detrital mineral assemblages in the upper Chicamocha river basin, Colombia. *Appl. Clay Sci.* **2020**, *196*, 105576. [[CrossRef](#)]
10. Hoving, A.L.; Sander, M.; Bruggeman, C.; Behrends, T. Redox properties of clay-rich sediments as assessed by mediated electrochemical analysis: Separating pyrite, siderite and structural Fe in clay minerals. *Chem. Geol.* **2017**, *457*, 149–161. [[CrossRef](#)]
11. Hu, S.Y.; Evans, K.; Fisher, L.; Rempel, K.; Craw, D.; Evans, N.J.; Cumberland, S.; Robert, A.; Grice, K. Associations between sulfides, carbonaceous material, gold and other trace elements in polyframboids: Implications for the source of orogenic gold deposits, Otago Schist, New Zealand. *Geochim. Cosmochim. Acta* **2016**, *180*, 197–213. [[CrossRef](#)]
12. Cornell, R.M.; Schwertmann, U. *The Iron Oxides: Structure, Properties, Reactions, Occurrences, and Uses*, 2nd ed.; Wiley VCH: Weinheim, Germany, 2003.

13. Cosmidis, J.; Benzerara, K.; Morin, G.; Busigny, V.; Lebeau, O.; Jézéquel, D.; Noël, V.; Dublet, G.; Othmane, G. Biomineralization of iron-phosphates in the water column of Lake Pavin (Massif Central, France). *Geochem. Cosmochim. Acta* **2014**, *126*, 78–96. [[CrossRef](#)]
14. Watanabe, T.; Katayanagi, N.; Agbisit, R.; Llorca, L.; Yasukazu, H.; Susum, A. Influence of alternate wetting and drying water-saving irrigation practice on the dynamics of Gallionella-related iron-oxidizing bacterial community in paddy field soil. *Soil Biol. Biochem.* **2021**, *152*, 108064. [[CrossRef](#)]
15. Zhang, Q.; Chen, H.; Huang, D.; Xu, C.; Zhu, H.; Zhu, Q. Water managements limit heavy metal accumulation in rice: Dual effects of iron-plaque formation and microbial communities. *Sci. Total Environ.* **2019**, *687*, 790–799. [[CrossRef](#)]
16. Ji, Y.; Liu, P.; Conrad, R. Response of fermenting bacterial and methanogenic archaeal communities in paddy soil to progressing rice straw degradation. *Soil Biol. Biochem.* **2018**, *124*, 70–80. [[CrossRef](#)]
17. Muyzer, G.; Stams, A.J.M. The ecology and biotechnology of sulphate-reducing bacteria. *Nat. Rev. Microbiol.* **2008**, *6*, 441–454. [[CrossRef](#)]
18. Qi, M.H.; Ma, S.S.; Qu, K.M.; Xin, F.Y. The formation of sulfide in the marine sediments and its relationships to cultivation of shellfish. *Mar. Fish. Res.* **2004**, *25*, 85–89.
19. Niu, Z.S.; Pan, H.; Guo, X.P.; Lu, D.P.; Feng, J.N.; Chen, Y.R.; Tou, F.; Liu, M.; Yang, Y. Sulphate-reducing bacteria (SRB) in the Yangtze Estuary sediments: Abundance, distribution and implications for the bioavailability of metals. *Sci. Total Environ.* **2018**, *634*, 296–304. [[CrossRef](#)] [[PubMed](#)]
20. Kiran, M.G.; Pakshirajan, K.; Das, G. Heavy metal removal from multicomponent system by sulfate reducing bacteria: Mechanism and cell surface characterization. *J. Hazard. Mater.* **2017**, *324*, 62–70. [[CrossRef](#)]
21. Tarekegn, M.M.; Zewdu, F.; Iniyehu, A. Microbes used as a tool for bioremediation of heavy metal from the environment. *Cogent Food Agric.* **2020**, *6*, 1783174. [[CrossRef](#)]
22. Wolfenden, S.; Charnock, J.M.; Hilton, J.; Livens, F.R.; Vaughan, D.J. Sulfide species as a sink for mercury in lake sediments. *Environ. Sci. Technol.* **2005**, *39*, 6644–6648. [[CrossRef](#)]
23. Kühl, M.; Jørgensen, B.B. Microsensor measurements of sulfate reduction and sulfide oxidation in compact microbial communities of aerobic biofilms. *Appl. Environ. Microbiol.* **1992**, *58*, 1164–1174. [[CrossRef](#)] [[PubMed](#)]
24. White, C.; Shaman, A.K. An integrated microbial process for the bioremediation of soil contaminated with toxic metals. *Nat. Biotechnol.* **1998**, *16*, 572–575. [[CrossRef](#)]
25. Corpoboyacá; Corporación Autónoma Regional de Boyacá; Pedagogical and Technological University of Colombia. *Plan de Ordenación y Manejo Ambiental de la Cuenca Alta del Río Chicamocha*; Corpoboyacá—Corporación Autónoma Regional de Boyacá; Pedagogical and Technological University of Colombia: Boyacá, Colombia; Universidad Nacional de Colombia: Bogotá, Colombia, 2006.
26. Márquez, G.; Guillot, G. *Ecología y Efecto Ambiental de Embalses—Aproximación a Casos Colombianos*; Universidad Nacional de Colombia: Bogotá, Colombia, 2001; Volume 218.
27. Quevedo, C.P.; Jiménez-Millán, J.; Cifuentes, G.R.; Jiménez-Espinosa, R. Electron microscopy evidence of Zn bioauthigenic sulfides formation in polluted organic matter-rich sediments from the Chicamocha River (Boyacá-Colombia). *Minerals* **2020**, *10*, 673. [[CrossRef](#)]
28. Klindworth, A.; Pruesse, E.; Schweer, T.; Peplies, J.; Quast, C.; Horn, M.; Glöckner, F.O. Evaluation of general 16S ribosomal RNA gene PCR primers for classical and next-generation sequencing-based diversity studies. *Nucleic Acids Res.* **2013**, *41*, e1. [[CrossRef](#)] [[PubMed](#)]
29. Schmieder, R.; Edwards, R. Quality control and preprocessing of metagenomic datasets. *Bioinformatics* **2011**, *27*, 863–864. [[CrossRef](#)]
30. Caporaso, J.G.; Lauber, C.L.; Walters, W.A.; Berg-Lyons, D.; Lozupone, C.A.; Turnbaugh, P.J.; Fierer, N. Global patterns of 16S rRNA diversity at a depth of millions of sequences per sample. *Proc. Natl. Acad. Sci. USA* **2011**, *108*, 4516–4522. [[CrossRef](#)]
31. Callahan, B.J.; McMurdie, P.J.; Rosen, M.J.; Han, A.W.; Johnson, A.J.; Holmes, S.P. DADA2: High-resolution sample inference from Illumina amplicon data. *Nat. Methods* **2016**, *13*, 581–583. [[CrossRef](#)]
32. Quast, C.; Pruesse, E.; Yilmaz, P.; Gerken, J.; Schweer, T.; Yarza, P.; Peplies, J.; Glöckner, F.O. The SILVA ribosomal RNA gene database project: Improved data processing and web-based tools. *Nucleic Acids Res.* **2013**, *41*, 590–596. [[CrossRef](#)]
33. Manning, P.G.; Prepas, E.E.; Serediak, M.S. Pyrite and vivianite intervals in the bottom sediments of eutrophic Baptiste Lake, Alberta, Canada. *Can. Miner.* **1999**, *37*, 593–601.
34. García-Ruiz, J.M.; Otálora, F. Crystal Growth in Geology: Patterns on the Rocks. In *Handbook of Crystal Growth*; Nishinaga, T., Rudolph, P., Eds.; Elsevier: Amsterdam, The Netherlands, 2015; Volume II, pp. 1–43.
35. Berg, J.S.; Jézéquel, D.; Duverger, A.; Lamy, D.; Laberty-Robert, C.; Miot, J. Microbial diversity involved in iron and cryptic sulfur cycling in the ferruginous, low-sulfate waters of Lake Pavin. *PLoS ONE* **2019**, *14*, e0212787. [[CrossRef](#)]
36. Rothe, M.; Kleeberg, A.; Hupfer, M. The occurrence, identification and environmental relevance of vivianite in waterlogged soils and aquatic sediments. *Earth Sci. Rev.* **2016**, *158*, 51–64. [[CrossRef](#)]
37. Berg, J.S.; Duverger, A.; Cordier, L.; Laberty-Robert, C.; Guyot, F.; Miot, J. Rapid pyritization in the presence of a sulfur/sulfate-reducing bacterial consortium. *Sci. Rep.* **2020**, *10*, 8264. [[CrossRef](#)]
38. Duverger, A.; Berg, J.S.; Busigny, V.; Guyot, F.; Bernard, S.; Miot, J. Mechanisms of Pyrite Formation Promoted by Sulfate-Reducing Bacteria in Pure Culture. *Front. Earth Sci.* **2020**, *8*, 588310. [[CrossRef](#)]

39. Egger, M.; Jilbert, T.; Behrends, T.; Rivard, C.; Slomp, C.P. Vivianite is a major sink for phosphorus in methanogenic coastal surface sediments. *Geochim. Cosmochim. Acta* **2015**, *169*, 217–235. [[CrossRef](#)]
40. Dijkstra, N.; Slomp, C.P.; Behrends, T. Vivianite is a key sink for phosphorus in sediments of the Landsort Deep, an intermittently anoxic deep basin in the Baltic Sea. *Chem. Geol.* **2016**, *438*, 58–72. [[CrossRef](#)]
41. Wu, M.; Liu, J.; Gao, B.; Sillanpää, M. Phosphate substances transformation and vivianite formation in P-Fe containing sludge during the transition process of aerobic and anaerobic conditions. *Bioresour. Technol.* **2021**, *319*, 124259. [[CrossRef](#)] [[PubMed](#)]
42. Druschel, G.K.; Emerson, D.; Sutka, R.; Suchecki, P.; Luther III, G.W. Low-oxygen and chemical kinetic constraints on the geochemical niche of neutrophilic iron(II) oxidizing microorganisms. *Geochim. Cosmochim. Acta* **2008**, *72*, 3358–3370. [[CrossRef](#)]
43. Wu, Y.F.; Xing, P.; Liu, S.; Wu, Q.L. Enhanced Microbial Interactions and Deterministic Successions During Anoxic Decomposition of *Microcystis* Biomass in Lake Sediment. *Front. Microbiol.* **2019**, *10*, 2474. [[CrossRef](#)]
44. Chang, C.H.; Wei, C.C.; Lin, L.H.; Tu, T.H.; Liao, V.H.C. Humic acids enhance the microbially mediated release of sedimentary ferrous iron. *Environ. Sci. Pollut. Res.* **2016**, *23*, 4176–4184. [[CrossRef](#)]
45. Li, H.; Xing, P.; Wu, Q.L. Characterization of the bacterial community composition in a hypoxic zone induced by *Microcystis* blooms in lake Taihu, China. *FEMS Microbiol. Ecol.* **2012**, *79*, 773–784. [[CrossRef](#)] [[PubMed](#)]
46. Hou, Y.; Li, B.; Feng, G.; Zhang, C.; He, J.; Li, H.; Zhu, J. Responses of bacterial communities and organic matter degradation in surface sediment to *Macrobrachium nipponense* bioturbation. *Sci. Total Environ.* **2021**, *759*, 143534. [[CrossRef](#)] [[PubMed](#)]
47. Timmers, P.H.A.; Vavourakis, C.D.; Kleerebezem, R.; Damsté, J.S.S.; Muyzer, G.; Stams, A.J.M.; Sorokin, D.Y.; Plugge, C.M. Metabolism and Occurrence of Methanogenic and Sulfate-Reducing Syntrophic Acetate Oxidizing Communities in Haloalkaline Environments. *Front. Microbiol.* **2018**, *9*, 3039. [[CrossRef](#)] [[PubMed](#)]
48. Lacerda-Júnior, G.V.; Noronha, M.F.; Cabral, L.; Delforno, T.P.; de Sousa, S.T.P.; Fernandes-Júnior, P.I.; Melo, I.S.; Oliveira, V.M. Land Use and Seasonal Effects on the Soil Microbiome of a Brazilian Dry Forest. *Front. Microbiol.* **2019**, *10*, 648. [[CrossRef](#)]
49. Kim, K.; Samaddar, S.; Chatterjee, P.; Ramasamy, K.; Jeon, S.; Sa, T. Structural and functional responses of microbial community with respect to salinity levels in a coastal reclamation land. *Appl. Soil Ecol.* **2019**, *137*, 96–105. [[CrossRef](#)]
50. Polivkova, M.; Suman, J.; Strejcek, M.; Kracmarova, M.; Hradilova, M.; Filipova, A.; Cajthaml, T.; Macek, T.; Uhlík, O. Diversity of root-associated microbial populations of *Tamarix parviflora* cultivated under various conditions. *Appl. Soil Ecol.* **2018**, *125*, 264–272. [[CrossRef](#)]
51. Radhakrishnan, M.; Imchen, M.; Kaari, M.; Angamuthu, V.; Venugopal, G.; Shanmugasundaram, T.; Joseph, J.; Balagurunathan, R.; Kumavath, R. Metagenomic insights unveil the dominance of undescribed Actinobacteria in pond ecosystem of an Indian shrine. *Meta Gene* **2019**, *23*, 100639. [[CrossRef](#)]
52. Dedysh, S.N.; Ivanova, A.A. Planctomycetes in boreal and subarctic wetlands: Diversity patterns and potential ecological functions. *FEMS Microbiol. Ecol.* **2019**, *95*, fyy227. [[CrossRef](#)]
53. Lin, X.; Hetharua, B.; Lin, L.; Xu, H.; Zheng, T.; He, Z.; Tian, Y. Mangrove Sediment Microbiome: Adaptive Microbial Assemblages and Their Routed Biogeochemical Processes in Yunxiao Mangrove National Nature Reserve, China. *Microb. Ecol.* **2019**, *78*, 57–69. [[CrossRef](#)]
54. Cifuentes, G.R.; Jiménez-Millán, J.; Quevedo, C.P.; Gálvez, A.; Castellanos-Rozo, A.; Jiménez-Espinosa, R. Trace element fixation in sediments rich in organic matter from a saline lake in tropical latitude with hydrothermal inputs (Sochagota Lake, Colombia): The role of bacterial communities. *Sci. Total Environ.* **2021**, *762*, 143113. [[CrossRef](#)]
55. Iino, T.; Mori, K.; Uchino, Y.; Nakagawa, T.; Harayama, S.; Suzuki, K. *Ignavibacterium album* gen. nov., sp. nov., a moderately thermophilic anaerobic bacterium isolated from microbial mats at a terrestrial hot spring and proposal of *Ignavibacteria classis* nov. for a novel lineage at the periphery of green sulfur bacteria. *Int. J. Syst. Evol. Microbiol.* **2010**, *60*, 1376–1382. [[CrossRef](#)]
56. Hazra, C.; Kundu, D.; Chaudhari, A.; Jana, T. Biogenic synthesis, characterization, toxicity and photocatalysis of zinc sulfide nanoparticles using rhamnolipids from *Pseudomonas aeruginosa*, BS01 as capping and stabilizing agent. *J. Chem. Technol. Biotechnol.* **2013**, *88*, 1039–1048. [[CrossRef](#)]
57. Zampieri, B.D.B.; da Costa Andrade, V.; Chinellato, R.M.; Garcia, C.A.B.; de Oliveira, M.A.; Brucha, G.; Fernandes Cardoso de Oliveira, A.J. Heavy metal concentrations in Brazilian port areas and their relationships with microorganisms: Can pollution in these areas change the microbial community? *Environ. Monit. Assess.* **2020**, *192*, 512. [[CrossRef](#)]
58. Ming, H.; Jingfeng, F.; Liu, J.; Jie, S.; Zhiyi, W.; Yantao, W.; Dongwei, L.; Mengfei, L.; Tingting, S.; Yuan, J.; et al. Full-length 16S rRNA gene sequencing reveals spatiotemporal dynamics of bacterial community in a heavily polluted estuary, China. *Environ. Pollut.* **2021**, *275*, 116567. [[CrossRef](#)]
59. Tu, Y.T.; Chiang, P.C.; Yang, J.; Chen, S.H.; Kao, C.M. Application of a constructed wetland system for polluted stream remediation. *J. Hydrol.* **2014**, *510*, 70–78. [[CrossRef](#)]
60. Liu, X.; Zhou, L.; Hou, L.; Yang, Y.; Wu, D.; Meadows, M.; Li, Z.; Tong, C.; Gu, J. Occurrence and distribution of PAHs and microbial communities in nearshore sediments of the Knysna Estuary, South Africa. *Environ. Pollut.* **2020**, *270*, 116083. [[CrossRef](#)]
61. Li, C.H.; Yan, K.; Tang, L.S.; Jia, Z.J.; Li, Y. Change in deep soil microbial communities due to long-term fertilization. *Soil Biol. Biochem.* **2014**, *75*, 264–272. [[CrossRef](#)]
62. Geesink, P.; Wegner, C.E.; Probst, A.J.; Herrmann, M.; Dam, H.T.; Kaster, A.K.; Küsel, K. Genome-inferred spatio-temporal resolution of an uncultivated Roizmanbacterium reveals its ecological preferences in groundwater. *Environ. Microbiol.* **2020**, *22*, 726–737. [[CrossRef](#)] [[PubMed](#)]

63. Wang, H.; Guo, C.; Yang, C.; Lu, G.; Chen, M.; Dang, Z. Distribution and diversity of bacterial communities and sulfate-reducing bacteria in a paddy soil irrigated with acid mine drainage. *J. Appl. Microbiol.* **2016**, *121*, 13143. [[CrossRef](#)]
64. Zhang, L.; Wang, Z.; Cai, H.; Lu, W.; Li, J. Long-term agricultural contamination shaped diversity response of sediment microbiome. *J. Environ. Sci.* **2021**, *99*, 90–99. [[CrossRef](#)] [[PubMed](#)]
65. Sanchez-Andrea, I.; Triana, D.; Sanz, J.L. Bioremediation of acid mine drainage coupled with domestic wastewater treatment. *Water Sci. Technol.* **2012**, *66*, 2425–2431. [[CrossRef](#)] [[PubMed](#)]
66. Chen, H.; Xiao, T.; Ning, Z.; Li, Q.; Xiao, E.; Liu, Y.; Xiao, Q.; Lan, X.; Ma, L.; Lu, F. In-situ remediation of acid mine drainage from abandoned coal mine by filed pilot-scale passive treatment system: Performance and response of microbial communities to low pH and elevated Fe. *Bioresour. Technol.* **2020**, *317*, 123985. [[CrossRef](#)] [[PubMed](#)]
67. Zhang, R.; Liu, W.C.; Liu, Y.; Zhang, H.L.; Zhao, Z.H.; Zou, L.Y.; Shen, Y.C.; Lan, W.S. Impacts of anthropogenic disturbances on microbial community of coastal waters in Shenzhen, South China. *Ecotoxicology* **2020**, *30*, 1652–1661. [[CrossRef](#)] [[PubMed](#)]